

New scandium rhodium boride $\text{Sc}_4\text{Rh}_{17}\text{B}_{12}$ with a framework structure: synthesis, crystal structure, and properties

A. M. Alekseeva,^{a,b} A. Leithe-Jasper,^a Yu. Prots,^a W. Schnelle,^a Yu. Grin,^a and E. V. Antipov^{b*}

^aMax-Planck Institute for the Chemical Physics of Solids,
40 Nöthnitzer Straße, 01187 Dresden, Germany*

^bLomonosov Moscow State University, Department of Chemistry,
Leninskie Gory, 119992 Moscow, Russian Federation.
Fax: (+7) (495) 739 8482. E-mail: antipov@icr.chem.msu.ru

The new scandium rhodium boride $\text{Sc}_4\text{Rh}_{17}\text{B}_{12}$ was synthesized by arc-melting of the elements followed by annealing in inert atmosphere. The crystal structure of $\text{Sc}_4\text{Rh}_{17}\text{B}_{12}$ was solved using single crystal X-ray diffraction data. The structure can be described as a three-dimensional framework formed by trigonal prisms $[\text{BRh}_6]$ and $[\text{BRh}_5\text{Sc}]$ with isolated boron atoms inside the prisms and trigonal prisms $[\text{BRh}_5\text{B}]$ representing the coordination polyhedra of paired boron atoms. The temperature dependences of the magnetic susceptibility and specific resistance of $\text{Sc}_4\text{Rh}_{17}\text{B}_{12}$ revealed that the compound is a Pauli paramagnet and shows metal-like specific resistance.

Key words: $\text{Sc}_4\text{Rh}_{17}\text{B}_{12}$, synthesis, crystal structure.

Owing to the specific electronic structure, scandium is often assigned to rare earth elements. However, due to the small atomic radius of Sc ($r_{\text{Sc}} = 1.606 \text{ \AA}$)¹ close to the radii of alkaline earth metals (for example, $r_{\text{Mg}} = 1.600 \text{ \AA}$),¹ the crystal chemistry of scandium compounds is unique in many respects. Thus ternary scandium and platinum metal borides tend to exist as both structural analogs of rare earth element borides or compounds isostructural to complex magnesium borides and as unique structural types, which are often related to transition metal compounds.

At low boron content ($M/B > 4$, where M is the total quantity of metals in the compound, $M = \text{Sc} + \text{T}$) in Sc–T–B systems, where T = Ru, Rh, Re, Os, Ir, perovskite-like compounds $\text{ScT}_3\text{B}_{1-x}$,^{2–4} typical of lanthanide containing systems, are formed. These compounds can be considered as interstitial solid solutions containing boron in the octahedral cavities of ScT_3 intermetallics. As the boron content increases to the ratio $1 \leq M/B \leq 4$, phases with structures identical to the structures of the corresponding magnesium borides are formed (ScOs_3B_4 is isostructural to MgOs_3B_4 (see Ref. 5); $\text{Sc}_3(\text{Ir},\text{Rh})_5\text{B}_2$ (see Refs 6, 7) corresponds to the structural type of $\text{Ti}_3\text{Co}_5\text{B}_2$ (see Ref. 8) and is isostructural to $\text{Mg}_3\text{Rh}_5\text{B}_2$ (see Ref. 7)). Also, among the ternary scandium and platinum metal borides in the composition region of $1 \leq M/B \leq 2$, there are compounds that form their own types of structure. These structures are often derived

from ternary rare earth element borides and are formed as a result of change in the composition or distortions associated with the small atomic radius of scandium (ScIr_3B_4 ,⁹ ScOsB_2 ,¹⁰ ScIr_3B_2 ,¹¹ $\text{Sc}_2(\text{Os},\text{Ru})_5\text{B}_4$ (see Ref. 12)). In the boron-rich region, there exist phases Sc_2TB_6 ^{5,13–14} crystallizing in the Y_2ReB_6 structural type,¹⁵ which is frequently encountered among rare earth element borides.

Considerable researchers' interest has always been attracted by compounds of the ET_4B_4 class (E is a rare earth metal) in the Sc–T–B systems with $1 \leq M/B < 2$. The compounds ET_4B_4 were discovered in 1977 by the example of ternary rhodium borides ERh_4B_4 ^{16,17} corresponding to the CeCo_4B_4 structural type (see Ref. 18). On temperature decrease, the ERh_4B_4 phases either exhibit superconducting properties or transform into a magnetically ordered state, depending on E. Further studies of these compounds have shown that the phases ET_4B_4 exist for a broad range of rare earth metals and for T = Ru,¹⁹ Rh,^{16,17} Os,^{20,21} Ir (see Refs 20–23). Depending on the chosen combination of metals E and T, compounds ET_4B_4 crystallize in three topologically related structural types: NdCo_4B_4 ,²⁴ LuRu_4B_4 ,¹⁹ and CeCo_4B_4 (see Ref. 18). Ternary scandium borides with the structure of NdCo_4B_4 have not been obtained. Presumably, the NdCo_4B_4 structure is formed for rare earth metals with large radii (from La to Gd) and for heavy platinum metals (Os, Ir).^{21,22} The regions with similar compositions of the Sc–Os–B and Sc–Ir–B systems comprise compounds whose structures differ from ET_4B_4 in crystal chemical features. Among ternary scandium and plati-

* Max-Planck-Institut für Chemische Physik fester Stoffe, 40 Nöthnitzer Straße, 01187 Dresden, Deutschland.

num metal borides, only one representative of the ET_4B_4 class is known, namely, ScRu_4B_4 , which belongs to the LuRu_4B_4 structural type. This compound is a superconductor with a critical temperature of ~ 8 K (see Ref. 25). The CeCo_4B_4 structural type is found most often among the ternary Rh borides but systematic studies^{16,17} showed the absence of ScRh_4B_4 with a CeCo_4B_4 type structure in the Sc–Rh–B system. No information about the compounds existing in the Sc–Rh–B system at $1 \leq M/B < 2$ can be found in the literature as yet,²⁶ although in this case, one can expect the formation of structures topologically similar to ET_4B_4 but with deviation of the composition from the ideal one.

This paper is devoted to the synthesis and study of the crystal structure and properties of a new ternary scandium and rhodium boride $\text{Sc}_4\text{Rh}_{17}\text{B}_{12}$.

Results and Discussion

A single crystal of the $\text{Sc}_4\text{Rh}_{17}\text{B}_{12}$ phase suitable for X-ray diffraction was prepared from a ScRhB_4 sample in a systematic investigation of the Sc–Rh–B system. The synthesis of the purest sample from a stoichiometric mixture of the elements was performed using the composition found by crystal structure refinement based on X-ray diffraction data.

The powder X-ray diffraction data indicate that the purest sample of the $\text{Sc}_4\text{Rh}_{17}\text{B}_{12}$ phase was synthesized by annealing for 10 days at 1200°C with intermediate quenching and grinding. The powder X-ray diffraction pattern was indexed in the monoclinic system with the unit cell parameters $a = 9.1602(4)$ Å, $b = 10.7074(5)$ Å, $c = 16.0714(4)$ Å, $\beta = 100.886(4)^\circ$, which are consistent with single-crystal X-ray diffraction data. In addition, the X-ray diffraction pattern shows additional reflections that could not be identified. Analysis of the reflection intensities allows one to roughly estimate the overall content of impurities to be 10% w/w (Fig. 1). The use of more grindings, an increase in the annealing time, and temperature variation in the range of 1000 – 1250°C did not decrease the amount of the impurity. The phase composition of the $\text{Sc}_4\text{Rh}_{17}\text{B}_{12}$ sample was additionally determined by metallographic and energy dispersive X-ray (EDXS) analyses, which showed the presence of the major phase with a Sc : Rh ratio of $1 : 4.25(8)$ described by the formula $\text{Sc}_4\text{Rh}_{17}\text{B}_{12}$. In addition to the major phase, small inclusions of the impurity phase with a Sc : Rh ratio of $1 : 7.3(1)$ were found. The impurity may contain light elements (C, B). However, no data on a compound with this composition in either the binary Sc–Rh system or ternary Sc–Rh–(B,C) systems have been reported.²⁶

The crystal structure of $\text{Sc}_4\text{Rh}_{17}\text{B}_{12}$ determined using single crystal X-ray diffraction data can be described most clearly as a set of structural blocks, each being

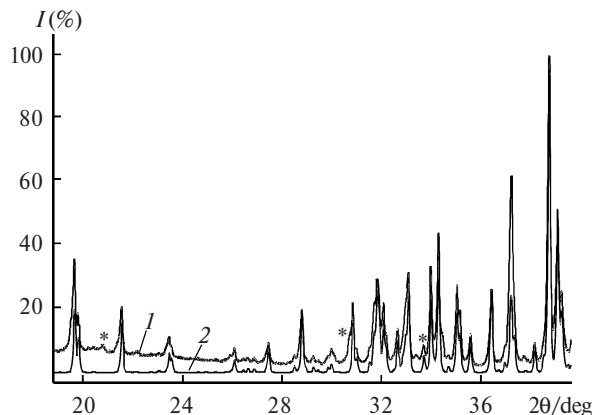


Fig. 1. Section of experimental (1) and theoretical (2) X-ray diffraction patterns of a $\text{Sc}_4\text{Rh}_{17}\text{B}_{12}$ sample. The diffraction maxima corresponding to the impurity are asterisked.

formed by a particular type of distorted trigonal prisms representing the boron coordination polyhedra.

In the structure of $\text{Sc}_4\text{Rh}_{17}\text{B}_{12}$, one can distinguish three topologically different types of trigonal prisms:

- (1) $[\text{B}'\text{Rh}_6]$ prisms formed only by platinum metal atoms and containing isolated boron atoms at the center;
- (2) $[\text{B}''\text{Rh}_5\text{Sc}'']$ prisms, which function as coordination polyhedra of isolated boron atoms but their vertices are occupied by scandium atoms in addition to rhodium;
- (3) interpenetrating $[\text{BRh}_5\text{B}]$ trigonal prisms of rhodium and boron atoms constituting the coordination environment of paired boron atoms.

The trigonal prisms of the first type $[\text{B}'\text{Rh}_6]$ are coordination polyhedra for the B(1), B(2), B(3), B(4), and B(5) atoms (Fig. 2, *a*). The interatomic distances from the vertices of the prism to the central atom are in the range of 2.10 – 2.39 Å. Fusion of the $[\text{B}'\text{Rh}_6]$ prisms through common vertices and edges gives rise to a three-dimensional framework (Fig. 3, *a*). A fragment of this framework illustrating different ways of connection of the $[\text{B}'\text{Rh}_6]$ prisms is shown in Fig. 3, *b*. The prisms around the B(4) atoms are connected in pairs by sharing a side edge, the pairs being arranged in such a way that the prism bases are nearly parallel to the (*ab*) plane (Fig. 3, *b*). In a similar way, rhodium atoms that occupy vertices of the prisms connected in pairs coordinate also the B(1) atoms. Every vertex of the prism around B(1) that does not belong to the shared side edge is connected to a prism with a B(2), B(3), or B(5) atom at the center. In turn, the prisms around B(2), B(3), and B(5) atoms are fused to form a block by sharing one vertex. It should be noted that connection of three prisms through a common vertex is rather seldom encountered in intermetallic structures. Among the broad range of structural types that can be described as a result of three-dimensional combination of trigonal-prismatic fragments (Fe_3C , Sc_3Co , Pd_5B_2 , Y_3Ni_2 , etc.), this mode of combination of prisms

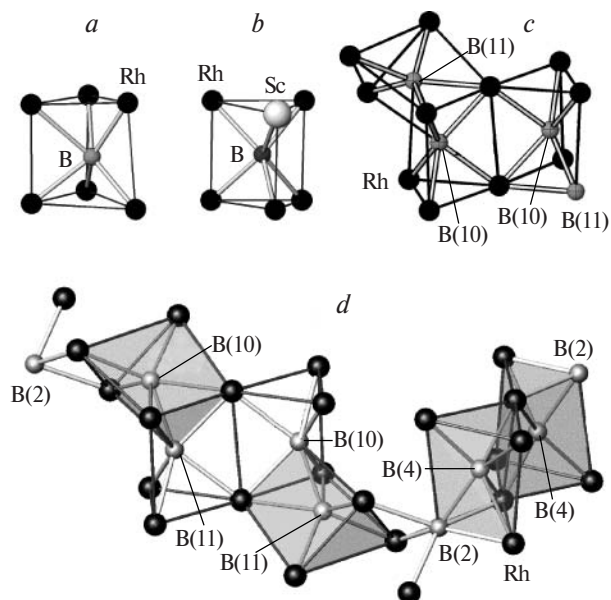


Fig. 2. Coordination polyhedra of boron atoms: (a) trigonal prism $[B'Rh_6]$, $B' = B(1), B(2), B(3), B(4), B(5)$; (b) trigonal prism $[B''Rh_5Sc'']$, $Sc'' = Sc(2), Sc(4)$; $B'' = B(6), B(7), B(8)$; (c) interpenetrating prisms $[BRh_5B]$, $B = B(9), B(10), B(11), B(12)$; (d) chain of interpenetrating prisms $[BRh_5B]$.

is present only in a Th_7Fe_3 type structure (see Ref. 27). The binary transition metal and platinum metal borides T_7B_3 ($T = Re, Ru, Rh$) are also representatives of this structural type.²⁸ Thus, in the crystal structure of the ternary compound $Sc_4Rh_{17}B_{12}$, one can distinguish a fragment of the binary boride Rh_7B_3 structure (see Fig. 3, c). Each prism having a B(3) atom at the center is connected through a common base edge with one prism from the pair around B(4). In addition, one prism of the pair around the B(4) atoms shares a vertex with the prism around B(5).

The trigonal prisms of the second type $[B''Rh_5Sc'']$ consist of five Rh atoms and one Sc'' atom (Fig. 2, b). The center of the $[B''Rh_5Sc'']$ prism is occupied by an isolated B(6), B(7), or B(8) atom (Fig. 4, a). Each $[B''Rh_5Sc'']$ prism typically has five shorter Rh–B'' distances (2.10–2.25 Å) and one longer Sc''–B'' distance (2.50–2.60 Å). The $[B''Rh_5Sc'']$ prisms form, in the $Sc_4Rh_{17}B_{12}$ structure, two-dimensional blocks (Fig. 4, b) approximately parallel to plane (011) and composed of groups of three prisms connected through common vertices (Fig. 4, a). Each group of three prisms is connected through two Rh and two Sc'' atoms to four neighboring groups. The trigonal prisms, $[B'Rh_6]$ and $[B''Rh_5Sc'']$, form together a complex three-dimensional framework being connected through common edges and faces of the bases.

Apart from the isolated boron atoms, the $Sc_4Rh_{17}B_{12}$ structure contains also boron atoms connected in pairs: B(9)–B(10) (1.89 Å) and B(11)–B(12) (1.90 Å). The

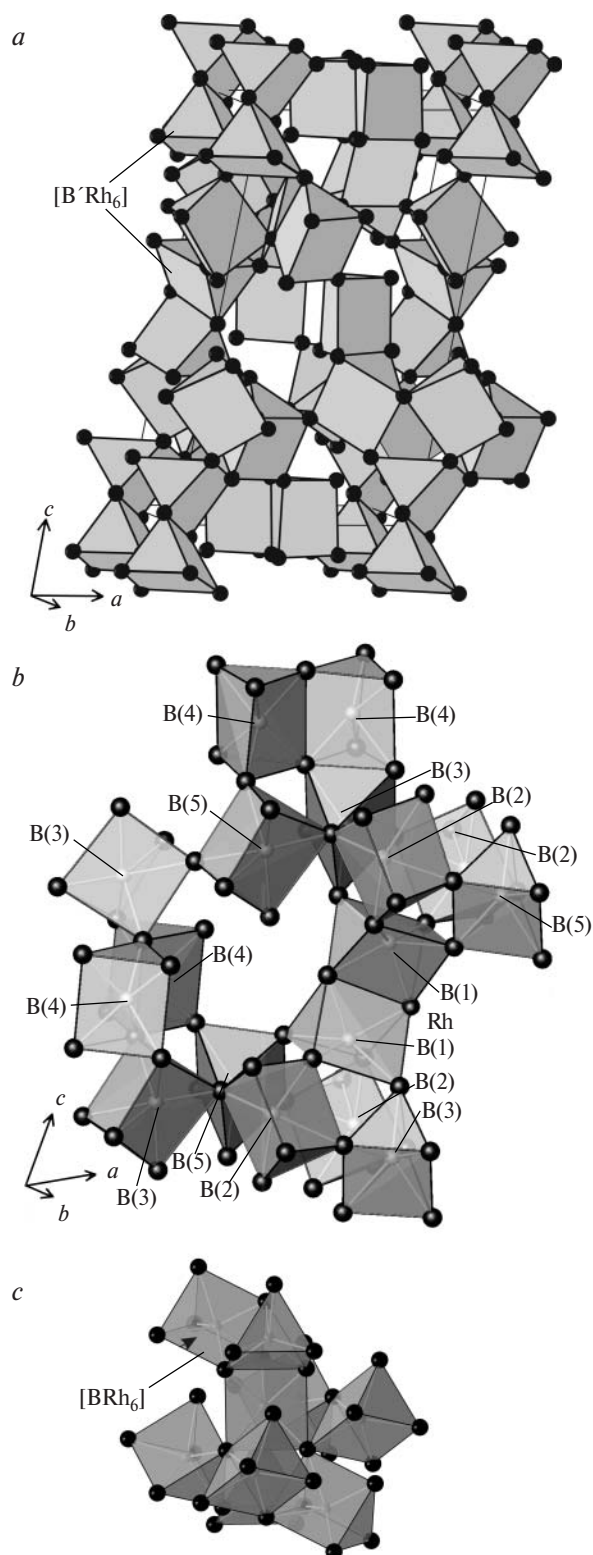


Fig. 3. Crystal structure of $Sc_4Rh_{17}B_{12}$ in the polyhedral representation (a) three-dimensional framework of trigonal prisms $[B'Rh_6]$, $B' = B(1), B(2), B(3), B(4), B(5)$; (b) fragment of the framework of trigonal prisms $[B'Rh_6]$ demonstrating various modes of connection of the prisms; (c) fragment of the framework of trigonal prisms $[BRh_6]$ in the structure of Rh_7B_3 .

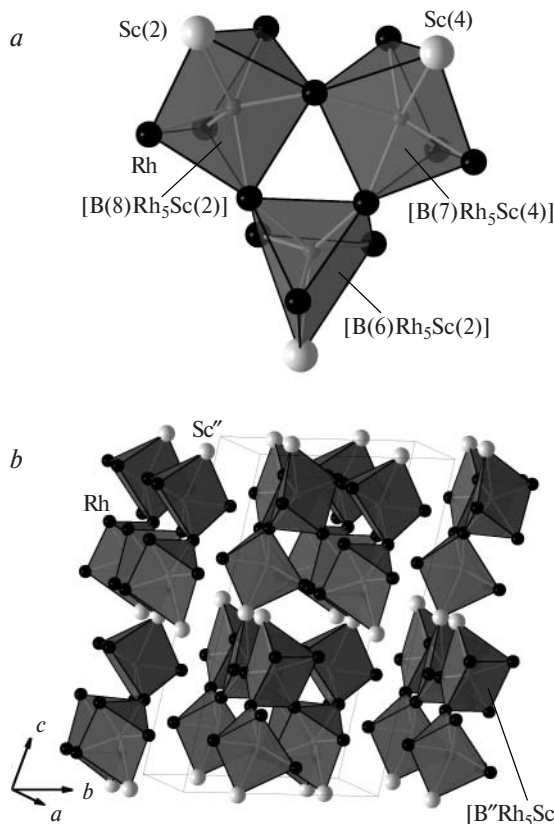


Fig. 4. Key element of a layer of trigonal prisms $[\text{B}''\text{Rh}_5\text{Sc}'']$ (a) and two-dimensional layers of trigonal prisms $[\text{B}''\text{Rh}_5\text{Sc}'']$ (b), $\text{Sc}'' = \text{Sc}(2), \text{Sc}(4)$; $\text{B}'' = \text{B}(6), \text{B}(7), \text{B}(8)$, in the structure of $\text{Sc}_4\text{Rh}_{17}\text{B}_{12}$.

local coordination environment of these boron atoms can be represented as interpenetrating trigonal prisms whose vertices are occupied by five rhodium atoms located at distances of 2.09–2.31 Å from the central boron atom and by one boron atom paired with the central boron atom (Fig. 2, *c, d*). The interpenetrating $[\text{BRh}_5\text{B}]$ prisms represent the third type of trigonal prisms present in the $\text{Sc}_4\text{Rh}_{17}\text{B}_{12}$ structure. They form chains extended along the (110) plane and alternating in the mutual arrangement along the direction *c* (Fig. 5, *a, b*).

The general view of the crystal structure of $\text{Sc}_4\text{Rh}_{17}\text{B}_{12}$ is shown in Fig. 6. The structure can be described as a 3D framework of trigonal prisms, $[\text{B}'\text{Rh}_6]$ (where $\text{B}' = \text{B}(1), \text{B}(2), \text{B}(3), \text{B}(4), \text{B}(5)$) and $[\text{B}''\text{Rh}_5\text{Sc}'']$ (where $\text{Sc}'' = \text{Sc}(2), \text{Sc}(4)$; $\text{B}'' = \text{B}(6), \text{B}(7), \text{B}(8)$) connected by sharing edges, vertices, and bases. Additionally, the trigonal prisms whose vertices are occupied by metal atoms are connected within the framework by short Rh–B and B–B distances (B(9), B(10), B(11), and B(12) atoms) (the short Rh–B distances correspond to interatomic distances between the paired boron atoms and Rh atoms functioning as vertices of the $[\text{B}'\text{Rh}_6]$ and $[\text{B}''\text{Rh}_5\text{Sc}'']$ prisms). The framework voids accommodate Sc(1) and Sc(3) atoms.

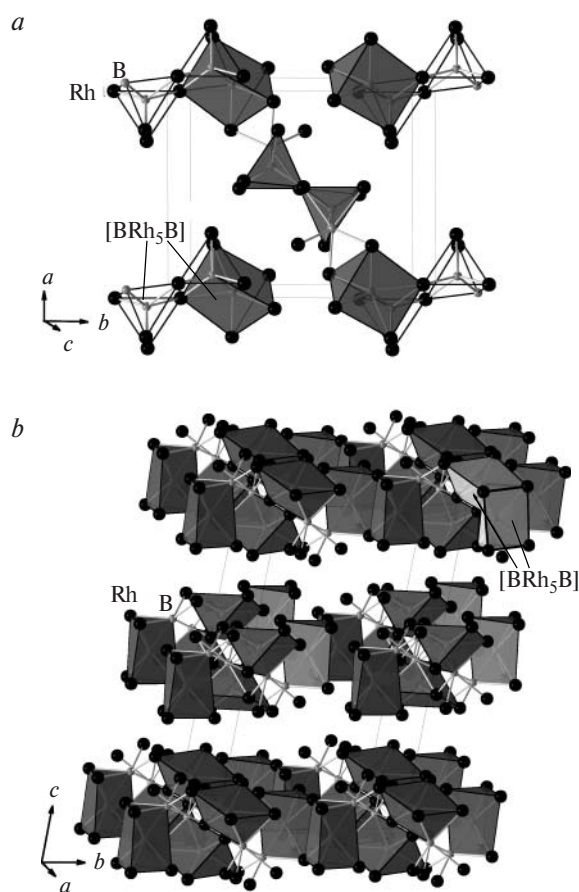


Fig. 5. Chains of $[\text{BRh}_5\text{B}]$ prisms extended along (110) (a) and two-dimensional layers of interpenetrating trigonal prisms $[\text{BRh}_5\text{B}]$ (b), $\text{B} = \text{B}(9), \text{B}(10), \text{B}(11), \text{B}(12)$, in the structure of $\text{Sc}_4\text{Rh}_{17}\text{B}_{12}$.

The coordination polyhedra of metal atoms in the $\text{Sc}_4\text{Rh}_{17}\text{B}_{12}$ structure can be described as complex 10–14-vertex polyhedra. The coordination polyhedra of the Sc(1)–Sc(4) atoms are shown in Fig. 7, *a–d*. They are formed by Rh atoms. The coordination environment of Sc(2) and Sc(4) atoms, each occupying a vertex of a $[\text{B}''\text{Rh}_5\text{Sc}'']$ trigonal prism, includes additionally the B'' atoms. The coordination polyhedra of rhodium are formed by four boron atoms, three scandium atoms, and 5–7 Rh atoms. As an example, Fig. 7, *e* shows the Rh(1) polyhedron. Only the Rh(17) atom does not have neighboring rhodium atoms in the local coordination sphere (Fig. 7, *f*).

The structure of $\text{Sc}_4\text{Rh}_{17}\text{B}_{12}$ (in which the ratio of the total amount of metals to borons $M/\text{B} = 1.75$) can be considered as a structure of new type quite unusual for compounds in the Sc–T–B system. Most often, the structures of complex transition element borides with atomic metal to boron ratio of $1 \leq M/\text{B} < 2$ contain pairs of and/or isolated boron atoms and are classified from the standpoint of boron coordination polyhedra. The topology of structural units formed by boron atoms and the type of coordina-

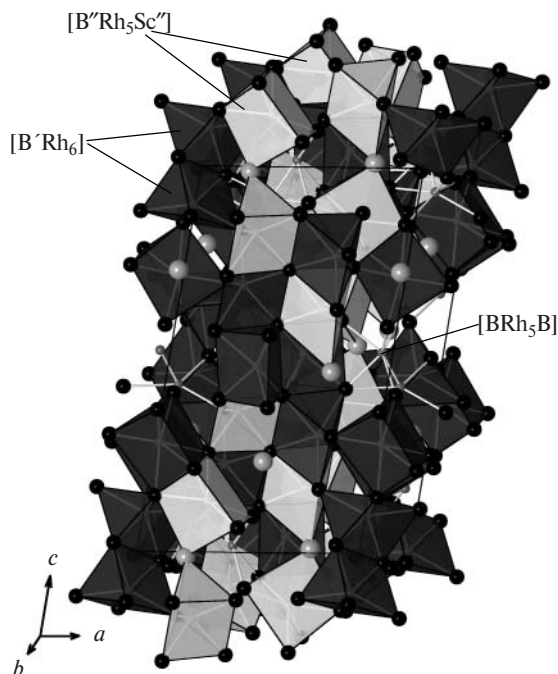


Fig. 6. General view of the crystal structure of $\text{Sc}_4\text{Rh}_{17}\text{B}_{12}$ as a three-dimensional framework of fused trigonal prisms $[\text{B}'\text{Rh}_6]$, $[\text{B}''\text{Rh}_3\text{Sc}'']$, and $[\text{BRh}_3\text{B}]$.

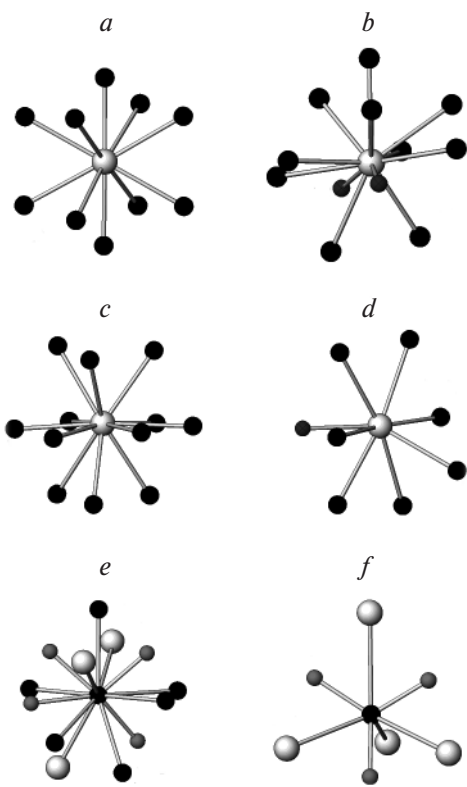


Fig. 7. Coordination polyhedra of metal atoms in the crystal structure of $\text{Sc}_4\text{Rh}_{17}\text{B}_{12}$: Sc(1) (a), Sc(2) (b), Sc(3) (c), Sc(4) (d), Rh(1) (e), Rh(17) (f).

tion polyhedra present correlate with the M/B ratio. By examining the published data on the ternary compounds in the Sc—T—B systems (T = Ru, Rh, Os, Ir, Re), one can discover some trends in the crystal chemistry of scandium and platinum metal ternary borides.

At $4 \geq \text{M/B} \geq 2$, the structures of complex scandium and platinum metal borides contain isolated boron atoms whose coordination spheres are $[\text{BT}_6]$ trigonal prisms. By being connected through common edges and faces of the base, $[\text{BT}_6]$ prisms form layers or 3D frameworks depending on the boron content. This type of structures include $\text{Sc}_3\text{Ir}_5\text{B}_2$, $\text{Sc}_3\text{Rh}_5\text{B}_2$ (see Refs 6 and 7) ($\text{M/B} = 4$, Fig. 8, a), and ScIr_3B_2 ¹¹ ($\text{M/B} = 2$, Fig. 8, b), the last-mentioned structure being a result of monoclinic distortion of a CeCo_3B_2 type structure,²⁹ which is common among ternary rare earth element borides.

As the M/B ratio decreases to 1.75, the isostructural compounds $\text{Sc}_2\text{Ru}_5\text{B}_4$ and $\text{Sc}_2\text{Os}_5\text{B}_4$ (see Ref. 12) retain the trigonal-prismatic coordination of boron atoms, $[\text{BT}_6]$; however, apart from isolated boron atoms, paired boron atoms appear (Fig. 8, c).

A further increase in the boron content to $\text{M/B} = 1.25$ leads to the a disturbance of the trigonal-prismatic coordination of boron atoms only by platinum metal atoms, resulting in the formation of a common 3D (T,B)-framework through B—B and T—B contacts. A similar coordination of boron atoms can be found in the structures of ET_4B_4 borides corresponding to the CoCo_4B_4 and LuRu_4B_4 structural types, represented, for example, by ScRu_4B_4 (see Ref. 25). The structures of CoCo_4B_4 and LuRu_4B_4 have always been described in terms of the traditional geometric views as packings of the $[\text{T}_4]$ tetrahedra and boride pairs. However, analysis of the interatomic distances shows that the T—T distances between the metal atoms in a framework of $[\text{T}_4]$ tetrahedra do not exceed $2r_{\text{T}}$. In addition, for every boron atom, one can distinguish six short distances, specifically, five T—B distances, which are shortened compared to the sum of the atomic radii, and one B—B distance (see Ref. 19). Data on the electron localization function studies of the chemical bonds in platinum metal borides^{30,31} show that the T—B distances correspond to the presence of a covalent or ionic T—B bond, indicating, for example, the formation of polyanions of B and T atoms. Consideration of the coordination of boron atoms in the structures of CeCo_4B_4 and LuRu_4B_4 based on five shorter T—B distances and one B—B distance in the pair results in a trigonal-prismatic coordination of each boron atom. Thus, the structures of CeCo_4B_4 and LuRu_4B_4 can be described as 3D frameworks of interpenetrating $[\text{BT}_5\text{B}]$ prisms (Fig. 8, d) similar to the prisms in the structure of $\text{Sc}_4\text{Rh}_{17}\text{B}_{12}$ (see Fig. 2, d).

When the ratio $\text{M/B} \leq 1$, 1D chains and 2D ribbons and layers of boron atoms appear in the structures of the Sc—T—B compounds, for example, structures ScIr_3B_4 ,⁹

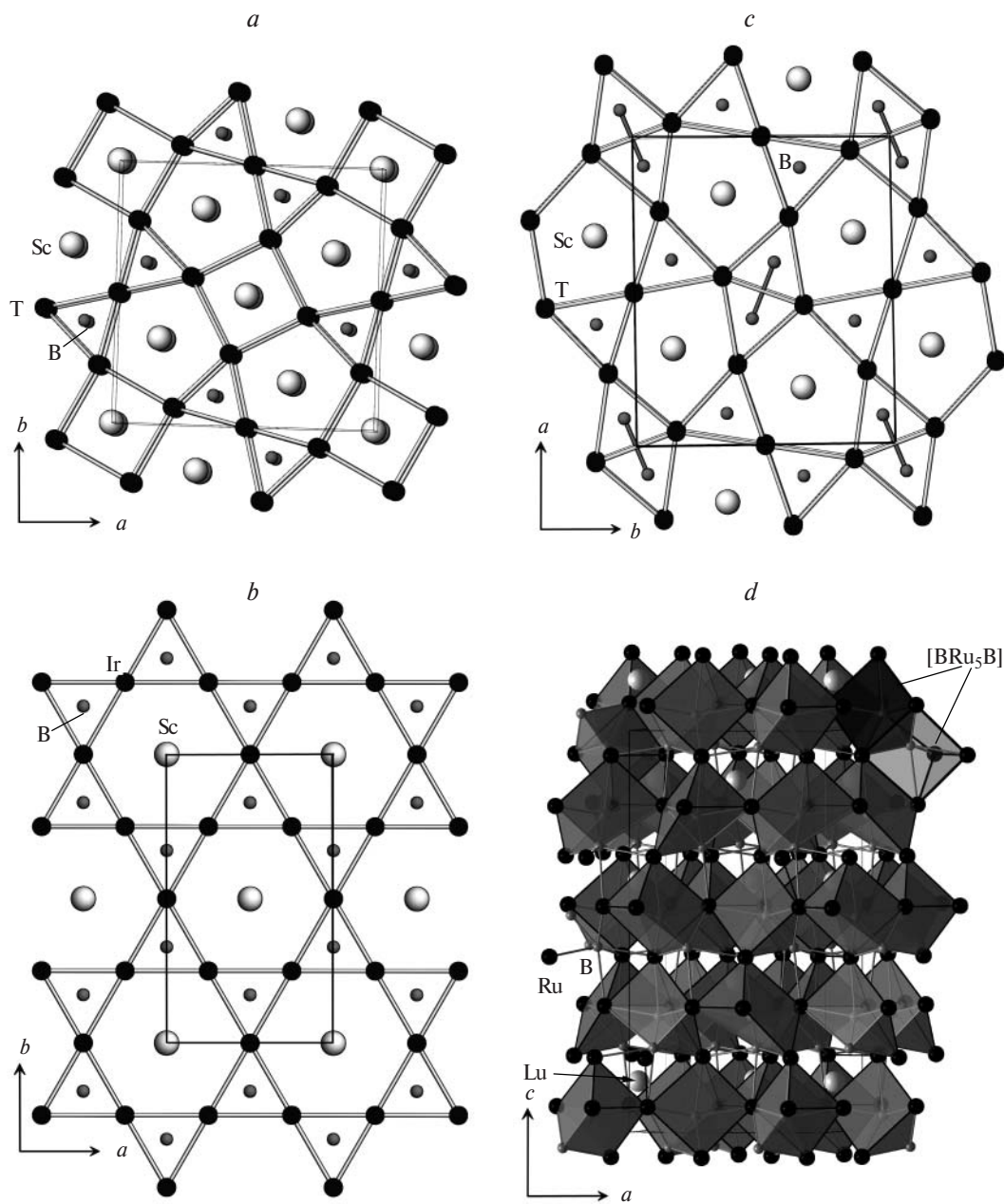


Fig. 8. Crystal structures of ternary borides in the Sc—T—B systems formed at $4 \geq M/B > 1$: $\text{Sc}_3\text{T}_5\text{B}_2$, T = Ir, Rh (a); ScIr_3B_2 (b); $\text{Sc}_2\text{Ru}_5\text{B}_4$ or $\text{Sc}_2\text{Os}_5\text{B}_4$ (c); LuRu_4B_4 (d).

ScOs_3B_4 ,⁵ ScOsB_2 ,¹⁰ and $\text{Sc}_2(\text{Rh},\text{Ir})\text{B}_6$ (see Refs 5, 13, 14).

Thus, the structure of $\text{Sc}_4\text{Rh}_{17}\text{B}_{12}$ can be represented as a set of structural fragments typical of ternary scandium and platinum metal borides with similar compositions (Table 1). Like the structures of $\text{Sc}_2\text{Ru}_5\text{B}_4$, $\text{Sc}_2\text{Os}_5\text{B}_4$ ($M/B = 1.75$), and ScIr_3B_2 ($M/B = 2$), the structure of $\text{Sc}_4\text{Rh}_{17}\text{B}_{12}$ contains a 3D framework of trigonal prisms with isolated boron atoms at their centers. However, in $\text{Sc}_4\text{Rh}_{17}\text{B}_{12}$, the framework is much more complicated and, apart from the $[\text{BT}_6]$ prisms, it contains prisms

formed by not only platinum metal atoms but also a Sc atom. In addition, the structure of $\text{Sc}_4\text{Rh}_{17}\text{B}_{12}$ also contains paired boron atoms whose coordination environment is formed by interpenetrating $[\text{BRh}_5\text{B}]$ prisms. Similar interpenetrating prisms, $[\text{BT}_5\text{B}]$, can be found in the borides ET_4B_4 ($M/B = 1.25$) corresponding to the CeCo_4B_4 and LuRu_4B_4 structural types. In $\text{Sc}_4\text{Rh}_{17}\text{B}_{12}$, the trigonal prisms $[\text{BRh}_5\text{B}]$ form 2D fragments, unlike the 3D frameworks present in ScRu_4B_4 .

Measurements of the temperature dependence of the magnetic susceptibility have shown that $\text{Sc}_4\text{Rh}_{17}\text{B}_{12}$ is

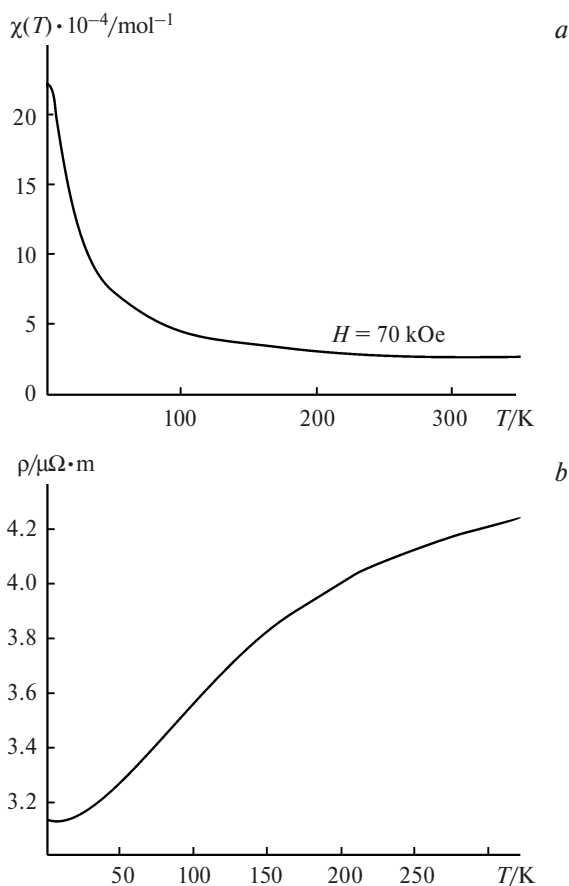
Table 1. Brief characteristics of known structures of ternary borides in the Sc–T–B systems (T = Ru, Rh, Ir, Os) formed at the metal (M = Sc + T) to boron atomic ratio of $4 \geq M/B > 1$

Compound	M/B	B atoms	Boron CP*	Refs
Sc ₃ (Ir,Rh) ₅ B ₂	4	Isolated	[B(Ir,Rh) ₆]	6, 7
ScIr ₃ B ₂	2	Isolated	[BIr ₆]	11
Sc ₂ (Ru,Os) ₃ B ₄	1.75	Isolated		
Sc ₄ Rh ₁₇ B ₁₂	1.75	and B–B pairs	[B(Ru,Os) ₆]	12
		Isolated and B–B pairs	[BRh ₆], [BRh ₅ Sc] [BRh ₅ B]	**
ScRu ₄ B ₄	1.25	B–B pairs	[BRu ₅ B]	25

* Coordination polyhedra of boron atoms.

** This work.

a Pauli paramagnet with a temperature-independent magnetic susceptibility component $\chi_0 = 1.7(1) \cdot 10^{-4} \text{ mol}^{-1}$ (Fig. 9, *a*). This fact attests to a metallic nature of the conduction of this compound and is in good agreement with the data on temperature dependence of the specific resistance of Sc₄Rh₁₇B₁₂ (Fig. 9, *b*). The results are consistent with the expected properties of

**Fig. 9.** Magnetic susceptibility (*a*) and specific resistance (*b*) of compound Sc₄Rh₁₇B₁₂ vs. temperature.

a ternary boride with relatively high metal content (63.6%). The compound does not show a superconducting transition down to 1.8 K (in a 20 Oe field).

Experimental

Scandium chips purified by distillation (Hunan Institute, 99.999%), Rh powder (Chempur, 99.9%), and crystalline boron (Alfa Aesar, 99.999%) were used as the initial chemicals. The presence of oxygen- and carbon-containing impurities in the initial Rh and B powders and transition metal impurities (Fe, Co, Ni, Ti, Mn, Mo, W) was determined by high-temperature flow gas extraction (combined infrared detector and katharometer, TC 436 DR/5, LECO, USA). According to the analysis, the O, C, and transition metal contents in the initial Rh and B powders were below the detection limit of $\leq 0.05\%$ (w/w). Due to the low reactivity of the crystalline boron, only the fraction with particle size of $< 25 \mu\text{m}$ obtained by sieving commercially available crystalline boron powder was used in the synthesis.

All operations on sample preparation were carried out under controlled argon atmosphere (the H₂O and O₂ contents ≤ 0.1 ppm). The samples were synthesized in several stages. First, a stoichiometric mixture of Rh and B (Rh : B = 17 : 12) was mixed in an agate mortar and pressed into a pellet. The pellet was arc-melted in argon atmosphere with a nonconsumable tungsten electrode on a water-cooled copper plate. Then the sample was fused together with a stoichiometric amount of Sc chips. The weight loss during fusion found by weighing the pellets before and after fusion was minor (≤ 0.001 g for a total sample weight of 0.5 g). The X-ray diffraction patterns of the samples after fusion showed incomplete reaction, as together with the desired phase, the samples contained considerable amounts of unreacted metals. To carry out homogenizing annealing, the resulting alloys were ground in an inert atmosphere in a tungsten carbide mortar, pressed into pellets, and welded into tantalum containers (20 mm long and 8 mm in diameter). The metallic containers were sealed in evacuated quartz tubes and annealed at 1000–1200 °C for 7–10 days with intermediate grindings. After annealing, the samples were cooled by water quenching.

Powder X-ray diffraction analysis was carried out at room temperature by the Guinier method (Image Plate Huber G670 camera, CuK α_1 radiation, $\lambda = 1.540598 \text{ \AA}$) using LaB₆ ($a = 4.15690 \text{ \AA}$) as the internal standard. The powder X-ray diffraction data were processed using WinXPow³² and WinCSD³³ software and the database PDF-2.³²

The single crystals of Sc₄Rh₁₇B₁₂ were prepared from a ScRhB₄ sample. This sample was obtained by arc-melting. After grinding and pressing into a pellet, the alloy was placed into a tantalum tube and heated to 1250 °C over a period of 3 days. The sample was kept at this temperature for 12 days and cooled by quenching of the tube in water. The single-crystal X-ray diffraction intensities were collected on a Rigaku AFC 7 automated diffractometer (Mercury CCD detector). The unit cell parameters were first determined by indexing of reflections obtained from X-ray experiment ($a = 9.1626(6) \text{ \AA}$, $b = 10.7087(5) \text{ \AA}$, $c = 16.098(1) \text{ \AA}$, $\beta = 100.86(3)^\circ$) and refined from powder X-ray diffraction data ($a = 9.1602(4) \text{ \AA}$, $b = 10.7074(5) \text{ \AA}$, $c = 16.0714(4) \text{ \AA}$, $\beta = 100.886(4)^\circ$). The crystallographic parameters and selected X-ray experiment details are summarized in Table 2. The absorption correction was applied by optimizing the crystal shape upon comparison of equivalent reflection intensities of a given Laue class.

Table 2. Crystal data and single crystal X-ray experiment details for Sc₄Rh₁₇B₁₂

Parameter	Value
Formula	Sc ₄ Rh ₁₇ B ₁₂
Molecular mass	2058.94
System	Monoclinic
Space group	<i>P</i> ₂ ₁ / <i>c</i>
<i>a</i> /Å ^a	9.1602(4)
<i>b</i> /Å	10.7074(5)
<i>c</i> /Å	16.0714(4)
β/deg	100.886(4)
<i>V</i> /Å ³	1547.9(2)
<i>Z</i>	4
Radiation	MoKα
λ/Å	0.71073
sinθ/λ	0.74
<i>d</i> _{calc} /g cm ⁻³	8.83
μ/cm ⁻¹	1599.52
The number of measured reflections	12616
The number of independent reflections	4505
<i>R</i> _{eq}	0.038
The number of reflections used in the refinement (<i>F</i> (<i>hkl</i>) ≥ 4σ(<i>F</i>))	3871
The number of refined parameters	239
The extinction coefficient ^b	0.00021
<i>R</i> (<i>F</i>), <i>R</i> (<i>F</i> ²) for <i>F</i> (<i>hkl</i>) ≥ 4σ(<i>F</i>) ^a	0.039, 0.040

^a The crystal lattice parameters were obtained from powder X-ray diffraction data.

^b The extinction coefficient was refined using the formula $k[1 + 0.001Fc^2\lambda^3/\sin(2\theta)]^{-1/4}$ (see Ref. 35).

Analysis of systematic extinctions (*h*0*l*: *l* ≠ 2*n*; 0*k*0: *k* ≠ 2*n*) indicated only one space group possible in the monoclinic system, namely, *P*₂₁/*c* (No. 14). At an initial stage, the crystal structure of Sc₄Rh₁₇B₁₂ was solved by the direct method using the SHELX97 program package,³⁵ and this was used to determine the positions of Rh atoms. Subsequently, the coordinates of the Sc and B atoms were determined by Fourier syntheses and difference Fourier syntheses. The final structure refinement was carried out using WinCSD software in the anisotropic approximation for atomic displacement parameters (Rh and Sc atoms). For boron atoms, due to the relatively small scattering factors, atomic displacement parameters were refined in the isotropic approximation. The positional atomic parameters in the structure of Sc₄Rh₁₇B₁₂ and isotropic parameters were deposited with the Inorganic Crystal Structure Database (ICSD). The anisotropic atomic displacement parameters and selected interatomic distances for Sc₄Rh₁₇B₁₂ are given in the supplementary material.

The metallographic investigation of the samples was carried out in reflected and polarized light using a Zeiss Axiotec 100 optical microscope. The content of Sc and Rh in the regions corresponding to homogeneous contrast region was analyzed by EDXS (a Philips XL30 scanning electron microscope, accelerating voltage 25 kV, a EDAX Phoenix EDXS detector) using Sc_K and Rh_L spectral lines.

The temperature dependence of the magnetic susceptibility was measured by a Quantum Design SQUID MPMS-XL7 magnetometer. A number of measurements in different magnetic fields (20 to 70 kOe) in the temperature range of 1.8–400 K were carried out.

A study of the magnetic susceptibility variation vs. field intensity was used to determine the presence of small amounts of paramagnetic and ferromagnetic impurities; in the determination of the temperature-independent component χ₀, appropriate corrections were applied.

The temperature dependence of the specific resistance was measured by a standard four-probe technique in the temperature range of 3.8–320 K.

The authors are grateful to U. Burkhardt, K. Schulze, and M. Eckert for performing metallographic and EDXS studies, to H. Auffermann and U. Schmidt for performing chemical analysis, and to A. M. Abakumov and P. S. Chizhov for discussion of the paper.

This work was supported by the Max Planck Society and the Russian Foundation for Basic Research (Project No. 06-03-33066).

References

1. J. Emsley, *The Elements*, Clarendon Press, Oxford, 1991.
2. H. Holleck, *J. Less-Common Metals*, 1977, **52**, 167.
3. T. Shishido, J. Ye, K. Kudou, S. Okada, T. Sasaki, S. Isida, T. Naka, M. Oku, I. Higashi, H. Kishi, H. Horiuchi, T. Fukuda, *J. Alloys. Compd.*, 2000, **309**, 107.
4. T. Shishido, J. Ye, K. Kudou, S. Okada, K. Obara, T. Sugawara, M. Oku, K. Wagatsuma, H. Horiuchi, T. Fukuda, *J. Alloys Compd.*, 1999, **291**, 52.
5. J. Schiffer, W. Jung, *J. Solid State Chem.*, 2000, **154**, 232.
6. E. A. Nagelschmitz, W. Jung, *Chem. Mater.*, 1998, **10**, 3189.
7. E. A. Nagelschmitz, W. Jung, R. Feiten, P. Müller, H. Lueken, *Z. Anorg. Allg. Chem.*, 2001, **627**, 523.
8. Yu. B. Kuz'ma, Ya. P. Yarmolyuk, *Zhurn. Strukt. Khim.*, 1971, **12**, 458 [*J. Struct. Chem. USSR*, 1971, **12** (Engl. Transl.)].
9. P. Rogl, H. Nowotny, *J. Less-Common Met.*, 1979, **67**, 41.
10. H. C. Ku, R. N. Shelton, *Mat. Res. Bull.*, 1980, **15**, 1445.
11. H. C. Ku, G. P. Meisner, *J. Less-Common Met.*, 1981, **78**, 99.
12. P. Rogl, *J. Solid State Chem.*, 1984, **55**, 262.
13. S. I. Mikhailenko, L. V. Zavaliy, Yu. B. Kuz'ma, L. I. Boiko Poroshkovaya Metallurgiya, 1991, **8(344)**, 67 [*Sov. Powder Metall. and Met. Ceramics*, 1992, **30**, 681 (Engl. Transl.)].
14. P. S. Salamakha, C. Rizzoli, L. P. Salamakha, O. L. Sologub, A. Gonzalves, M. Almeida, *J. Alloys Compd.*, 2005, **396**, 240.
15. Yu. B. Kuz'mina, S. I. Svarichevskaya, *Kristallografiya*, 1972, **17**, 658 [*Sov. Phys. Crystallogr.* 1972, **17**, 569 (Engl. Transl.)].
16. J. M. Vandenberg, B. T. Matthias, *Proc. Natl. Acad. Sci. USA*, 1977, **74**, 1336.
17. B. T. Matthias, E. Corenzwit, J. M. Vandenberg, H. E. Barz, *Proc. Natl. Acad. Sci. USA*, 1977, **74**, 1334.
18. Yu. B. Kuz'mina, N. S. Bilonizhko, *Kristallografiya*, 1971, **16**, 1030 [*Sov. Phys. Crystallogr.*, 1972, **16**, 897 (Engl. Transl.)].
19. D. C. Johnston, *Solid State Commun.*, 1977, **24**, 699.
20. K. Hiebl, P. Rogl, M. J. Sienko, *Inorg. Chem.*, 1982, **21**, 1128.
21. P. Rogl, *Monatsh. Chem.*, 1979, **110**, 235.
22. P. Rogl, *Monatsh. Chem.*, 1980, **111**, 517.
23. H. C. Ku, B. T. Matthias, H. Barz, *Solid State Commun.*, 1979, **32**, 937.
24. Yu. B. Kuz'ma, N. S. Bilonizhko, *Dopov. Akad. Nauk USSR, Ser. A [Bull. Ukr. Acad. Sci., Ser. A]*, 1978, **40**, 275.

25. H. C. Ku, D. J. Johnston, B. T. Matthias, H. Barz, G. Burri, L. Rinderer, *Mat. Res. Bull.*, 1979, **14**, 1591.
26. P. Rogl, *Handbook on the Physics and Chemistry of Rare Earth*, Ed. K. A. Gschneidner, Jr., L. Eyring, Elsevier Science Publishers B. V., 1984.
27. E. I. Gladyshevskii, Yu. N. Grin, *Kristallografiya*, 1981, **26**, 1204 [*Sov. Phys. Crystallogr.* (Engl. Transl.)].
28. B. Aronsson, E. Stenberg, J. Aselius, *Acta Chem. Scand.*, 1960, **14**, 733.
29. Yu. B. Kuz'ma, P. I. Krip'yakevich, N. S. Bilonizhko, *Dopov. Akad. Nauk USSR, Ser. A* [*Bull. Ukr. Acad. Sci., Ser. A*], 1969, **10**, 939.
30. A. M. Alekseeva, A. M. Abakumov, A. Leithe-Jasper, W. Schnelle, Yu. Prots, J. Hadermann, G. Van Tendeloo, E. V. Antipov, Y. Grin, *Z. Anorg. Allgem. Chem.*, 2005, **631**, 1047.
31. A. M. Alekseeva, A. M. Abakumov, A. Leithe-Jasper, W. Schnelle, Yu. Prots, P. S. Chizhov, G. Van Tendeloo, E. V. Antipov, Yu. Grin, *J. Solid State Chem.*, 2006, **179**, 751.
32. STOE WinXPow, Version 1.2, STOE and Cie GmbH, Darmstadt, Germany, 2000.
33. L. G. Akselrud, P. Yu. Zavalii, Yu. Grin, V. K. Pechar-sky, B. Baumgartner, E. Wölfel, *Mater. Sci. Forum*, 1993, **133–136**, 335.
34. Database PDF-2, International Center for Diffraction Data, Newton Square, USA, 1998.
35. G. M. Sheldrik, *SHELXS-97, Program for Crystal Structure Solution*, University of Göttingen, Göttingen, Germany, 1997.

*Received August 30, 2006;
in revised form October 17, 2007*